

1 ***Drosophila* macrophage self-renewal is regulated by transient expression of PDGF- and**  
2 **VEGF-related factor 2**

3

4

5 **Daniel Bakopoulos<sup>1</sup>, James C. Whisstock<sup>2,3</sup>, Coral G. Warr<sup>4</sup> and Travis K. Johnson<sup>1,2,5</sup>**

6

7 **Author affiliations:**

8 <sup>1</sup>School of Biological Sciences, Monash University, Clayton, Victoria 3800, Australia.

9 <sup>2</sup>Australian Research Council Centre of Excellence in Advanced Molecular Imaging,

10 <sup>3</sup>Department of Biochemistry and Molecular Biology, Monash University, Clayton, VIC  
11 3800, Australia.

12 <sup>4</sup>Tasmanian School of Medicine, University of Tasmania, Hobart, Tasmania 7000, Australia.

13 <sup>5</sup>Corresponding author. Travis K. Johnson, School of Biological Sciences, Monash  
14 University, Clayton, Victoria 3800, Australia. E-mail: [travis.johnson@monash.edu](mailto:travis.johnson@monash.edu), Phone:  
15 +613 9905 5620

16

17 **Key words:** *Drosophila melanogaster*, macrophage, plasmatocyte, hemocyte, hematopoiesis,  
18 PDGF, VEGF, Pvr, Pvf1, Pvf2, Pvf3

19 **Abstract**

20 Macrophages are an ancient animal blood cell lineage critical for tissue homeostasis and  
21 defence against pathogens. Until recently, their numbers were thought to be sustained solely  
22 by specialised hematopoietic organs. It is now clear that many macrophages are instead  
23 replenished by self-renewal, yet the signals that regulate this remain poorly understood. In  
24 *Drosophila melanogaster*, macrophages (known as plasmatocytes) undergo a phase of rapid  
25 population expansion via self-renewal, making *Drosophila* an attractive model for revealing  
26 the signals and regulatory mechanisms involved. However, no central self-renewal pathway  
27 has been identified in *Drosophila*. Here, we investigated the PDGF-/VEGF-receptor pathway  
28 as a candidate for playing this role. Analysis of larvae deficient for each of the three PDGF-  
29 /VEGF-receptor ligands *Pvf1-3* revealed *Pvf2* as a major driver of macrophage self-renewal  
30 in *Drosophila*. We further found that only a small proportion of blood cells express *Pvf2*, and  
31 knockdown experiments implicate these cells as a major source of *Pvf2* in self-renewal.  
32 Lineage tracing studies support the idea that *Pvf2* expression in blood cells occurs transiently  
33 throughout the macrophage self-renewal period, and in response to an as yet unidentified cue.  
34 These data define the regulation of *Pvf2* expression in blood cells as a central mechanism by  
35 which macrophage self-renewal is controlled. Given the strong parallels that exist between  
36 *Drosophila* and vertebrate macrophage systems, it is likely that similar mechanisms are at  
37 play across animal phyla.

## 38 **Introduction**

39           Macrophages are highly versatile blood cells that reside within body tissues and play  
40 critical roles in immune surveillance, pathogen and cellular debris clearance, inflammation,  
41 wound healing, and a variety of developmental processes (1-3). Macrophage numbers are  
42 highly dynamic during the lifetime of an animal. For example, their numbers increase upon  
43 infection as part of the immune response, while during development their populations expand  
44 rapidly in order to colonise growing tissues for important local homeostatic duties (1, 4-6).  
45 For many years, the vertebrate macrophage population was thought to be sustained solely by  
46 the contributions of blood cell progenitors and hematopoietic stem cells (HSCs). Recently  
47 however, it has become clear that the ability of macrophages to proliferate (or self-renew)  
48 locally within tissues also plays a major role (1, 7). Despite the importance of self-renewal to  
49 the macrophage population, the signals and pathways that control this process remain poorly  
50 understood (8, 9). Adding to the complexity is that often the vertebrate self-renewing  
51 macrophage populations coexist with those of HSC origins, thereby making the task of  
52 identifying novel self-renewal mechanisms challenging (10, 11).

53           The blood cell systems of many invertebrates, including *Drosophila melanogaster*,  
54 similarly comprise macrophages (called plasmatocytes) that arise de novo from blood cell  
55 progenitors or via self-renewal (12-14). In *Drosophila*, macrophages make up more than 90%  
56 of the total population of blood cells (known as hemocytes) (6). The remainder are crystal  
57 cells (<5%), responsible for protective melanisation reactions during infection, and  
58 lamellocytes, which appear upon wasp parasitisation to encapsulate wasp eggs (6, 15-17).

59           All *Drosophila* blood cells originate from two populations of blood cell progenitors  
60 (18, 19). During embryogenesis, the first blood cell progenitor population gives rise to both  
61 crystal cells and macrophages (12, 20). The latter persist into the larval stages where they can  
62 either circulate throughout the blood (called lymph) or reside in tissues termed hematopoietic

63 pockets (19-21). During the subsequent four days that constitute the larval stage, the  
64 macrophage population expands dramatically from several hundred cells to approximately  
65 10,000 via self-renewal (6, 13, 19, 22). During this time, crystal cells and lamellocytes arise  
66 from the macrophage pool via transdifferentiation (5, 23).

67         The second population of blood cell progenitors originate within a HSC-like niche in  
68 the larva called the lymph gland (14). The blood cells that are produced here, however, are  
69 not released into circulation until the onset of metamorphosis, which marks the completion of  
70 the larval stage (19, 24). This means that, unlike in vertebrates, the self-renewing  
71 macrophages in fly larvae are easily separated from those of HSC origin. For this reason,  
72 *Drosophila* is emerging as a useful model for the study of self-renewal mechanisms (11, 25).  
73 Despite this, a central cell signalling pathway responsible for driving macrophage self-  
74 renewal in remains *Drosophila* to be described. Thus, our understanding of the mechanism(s)  
75 by which this process is controlled remain incomplete.

76         A candidate for this is the PDGF- and VEGF-receptor related (Pvr) pathway. Pvr is a  
77 receptor tyrosine kinase with three known ligands, PDGF- and VEGF- related factors 1-3  
78 (Pvfs1-3), and is the sole *Drosophila* orthologue of the PDGF and VEGF family of receptors  
79 (26, 27). Pvr signalling has been previously implicated in the survival of blood cells during  
80 embryogenesis, and while it is thought to also influence larval blood cells, its role here has  
81 remained unclear (28-31). We therefore investigated the Pvr pathway and found it to be a  
82 major driver of macrophage self-renewal in *Drosophila*. We find that final larval macrophage  
83 numbers are drastically reduced in *Pvf2* and *Pvf3* mutants and show that *Pvf2* alone  
84 influences macrophage self-renewal. We further find that *Pvf2* is transiently expressed in  
85 only a small proportion of blood cells, and that its modulation here causes large and  
86 concomitant changes in their population size. These data support a new model for larval

87 macrophage self-renewal in *Drosophila* that involves the transient transcriptional regulation  
88 of *Pvf2* in blood cells.

89

## 90 **Materials and methods**

### 91 *Drosophila* stocks and maintenance

92 The following stocks from the Bloomington *Drosophila* Stock Centre were used: *w*<sup>1118</sup>  
93 (BL3605), *hml-GAL4,UAS-GFP* (BL6397), *hmlΔ-GAL4,UAS-GFP* (BL30142), *Pvfl*<sup>1624</sup>  
94 (BL11450), *Pvf2*<sup>M100770</sup> (BL32696), *Pvf3*<sup>M104168</sup> (BL37270; called *Pvf3*<sup>MiMIC</sup> here), *df*<sup>BSC291</sup>  
95 (BL23676), *UAS-Pvf2* (BL19631), *UAS-eYFP;Sp/CyO;Dr/TM3* (BL60291), *hs-Cre,vas-*  
96 *dφC31* (BL60299), *Sp/CyO;lox(Trojan-GAL4)x3* (BL60311), *SrpHemo-H2A-*  
97 *mCherry/CyO;Dr/TM3* (BL78361), *UAS-EOS-GFP* (BL32228), *UAS-FLP,UAS-RFP,Ubi*<sup>p63</sup>-  
98 *FRT-STOP-FRT-GFP* (BL28280, called *G-TRACE* here); *UAS-RFP* (BL8546). We obtained  
99 *UAS-Pvf2 RNAi* (13780R-1) from NIG Japan, and *UAS-eYFP* was derived from BL60291.  
100 T2A-GAL4 lines were generated via RMCE using BL60291, BL60299 and BL60311 as  
101 previously described (32). *Pvf2*<sup>T2A-GAL4</sup>, *Pvf3*<sup>MiMIC</sup>, *df*<sup>BSC291</sup>, *UAS-Pvf2* and *UAS-Pvf2 RNAi*  
102 were maintained over green (GFP) balancers. *hmlΔ-GAL4,UAS-GFP* was maintained over  
103 TM6B. *hmlΔdsRed* was a gift from Katja Brückner (13). Flies were raised and maintained on  
104 standard sucrose, yeast and semolina fly media. All experiments were performed at 25 °C.

105

### 106 Quantitative RT-PCR

107 RNA was extracted from the anterior half of wandering larvae using Trisure reagent (Bioline)  
108 and cDNA synthesised using oligodT and random hexamers (Bioline). Quantitative PCR was  
109 performed on a lightcycler (Roche) with SYBR chemistry. The following primers pairs were  
110 designed (PerlPrimer) (33), validated and tested for efficiency: *Pvf2*: F 5'-TGA AAG AGC  
111 GAA TCG CCG AAC AA-3' and R 5'-GCA GAT ACC CTC CTT TGC CAT CA-3', *Pvf3*:

112 F 5'-TCT ATA CGC CTC ACT GCA CCA TCC-3' and R 5'-ACT GCG ATG CTT ACT  
113 GCT CTT CAC-3'. Reactions for *Pvf2* and *Pvf3* and the control gene *cyclin K*: F-5'-GAG  
114 CAT CCT TAC ACC TTT CTC CT-3', R-5'-TAA TCT CCG GCT CCC ACT G-3' (34),  
115 were run in triplicate for 3-4 biological replicates per genotype and fold changes determined  
116 using the  $\Delta\Delta CT$  method. Differences between means were assessed using an unpaired t-test  
117 with Welsch's correction (Graphpad Prism 8).

118

### 119 Larva rearing and weighing

120 For wandering third instar larvae, 0-24 hour old larvae were collected from egg-lays on apple  
121 juice agar supplemented with yeast paste, then reared on standard fly media under non-  
122 crowded conditions until the wandering stage. Where newly moulted third instar larvae were  
123 needed, developing larval cultures were suspended with sucrose (20% w/vol) and second  
124 instar larvae placed onto fresh fly media based on their anterior spiracle morphology. This  
125 was repeated two hours later and the newly moulted third instar larvae used in experiments.  
126 For first instar larvae, 2 hour egg-lays were performed and individuals allowed to develop a  
127 further 44-46 hours on apple juice agar supplemented with yeast paste before bleeding.  
128 Correct genotypes were selected using balancers marked by GFP expression or Tb as  
129 required. To weigh larvae individual wandering third instar larvae were washed in phosphate  
130 buffered saline (PBS), checked for debris, blotted dry and weighed on an ultra-microbalance  
131 (XP2U, Mettler Toledo) immediately prior to bleeding.

132

### 133 Blood cell quantification

134 Blood cells were extracted from third instar wandering stage larvae (unless otherwise stated)  
135 carrying a fluorescent blood cell marker – *hml-GAL4,UAS-GFP* (35), *hml $\Delta$ -GAL4,UAS-GFP*  
136 (36) or *hml $\Delta$ dsRed* (13) – or *G-TRACE* transgenes as previously described (22). Briefly,

137 circulating blood cells were bled from individual larvae in PBS in an 8-well slide (Ibidi) for  
138 at least two minutes through from a hole torn in the dorsal-posterior cuticle. Tissue-resident  
139 blood cells were removed by scraping the remaining blood cells from the carcass into a new  
140 well, while taking care not to disrupt the lymph gland. Cells were resuspended by pipetting to  
141 minimise clumping and allowed to settle for at least 10 minutes. The entire well was imaged  
142 using an Olympus CV1000 for all experiments, except for the *Pvf2* knockdown experiment  
143 where a Leica AF6000 LX was used. The threshold feature on ImageJ was used to determine  
144 the number of relevant classes of fluorescent cells per well, applying the same threshold  
145 across all images in a given experiment (37). Differences between means were assessed using  
146 the non-parametric Mann-Whitney test (Graphpad Prism 8). When larval weights or stage  
147 differences were accounted for, regression analyses were performed following log  
148 transformation to ensure linearity across the data range (RStudio) as previously described  
149 (38).

150

151 Crystal cells were counted using the black cell assay (39). Briefly, wandering third instar  
152 larvae were placed into 100 $\mu$ L H<sub>2</sub>O and heated in a 65°C water bath for 20 minutes. Larvae  
153 were then stored in H<sub>2</sub>O at -20°C for no longer than 72 hours before being imaged on a Leica  
154 M165 FC. The number of crystal cells on the dorsal side of the four posterior-most  
155 abdominal segments were counted in ImageJ using the Cell Counter plugin for  $\geq 13$  larvae per  
156 genotype (37). Differences between means were assessed using the non-parametric Mann-  
157 Whitney test (Graphpad Prism 8).

158

### 159 Blood cell self-renewal and death measurements

160 Self-renewal rates were assayed by feeding newly moulted third instar larvae carrying  
161 *hml $\Delta$ dsRed* standard fly media containing 200 $\mu$ M 5-ethynyl-2'-deoxyuridine (EdU), 1:50

162 dimethyl sulfoxide (DMSO) and red food colouring for 4 hours prior to bleeding, as  
163 previously described (40). Larvae that had ingested food were selected and their blood cells  
164 extracted into a droplet of PBS on a Concanavalin A (ConA, 0.5mg/mL) coated coverslip and  
165 allowed to settle for 30 minutes. Blood cells were fixed and stained using the Click-iT EdU  
166 Proliferation Kit for Imaging (Invitrogen), imaged and quantified as described above. For cell  
167 death measurements, cells were bled from newly moulted third instar larvae and adhered to  
168 ConA coverslips. Bled cells were fixed and stained using TUNEL reagents (Roche) before  
169 imaging and quantification. Differences between means were assessed using the non-  
170 parametric Mann-Whitney test (Graphpad Prism 8).

171

#### 172 Embryonic blood cell imaging

173 Embryos were dechorionated for 3 minutes in 50% (vol/vol) bleach and fixed in a mixture of  
174 1:1 PBS containing 4% paraformaldehyde (PFA) and heptane for 30 minutes before methanol  
175 devitellinisation. Embryos were rehydrated in PBS containing 0.1% Triton X (PBS-T),  
176 blocked for 30 minutes in PBS-T with 5% (vol/vol) normal goat serum (G-9023, Sigma)  
177 before overnight incubation with anti-GFP (1:1000, A-6455 Invitrogen). Anti-rabbit  
178 secondary (1:500, A-11034 Invitrogen) was applied and embryos mounted in Vectashield  
179 before imaging. For live-imaging, embryos were dechorionated for 90 seconds and mounted  
180 in 8-well slides (Ibidi) under PBS for imaging.

181

#### 182 Lineage tracing with EOS-GFP and live imaging of larvae

183 Third instar larvae expressing EOS-GFP were irradiated in H<sub>2</sub>O using a DAPI filter and 5x  
184 objective (Leica DMLB compound) for at least 2 minutes to ensure high conversion  
185 efficiency while maximising larval survival. Larvae were then placed on standard fly media.



186 Larvae were imaged live 24 hours later, on a microscope slide held in place by double-sided  
187 tape under a coverslip (towards the dorsal side) as previously described (23).

188

## 189 **Results**

### 190 Larval macrophage number is influenced by *Pvf2* and *Pvf3*, but not *Pvf1*

191 To determine whether any of the three known Pvr ligands (*Pvf1-3*) may play a central  
192 role in the control of macrophage population expansion in larvae, we sought to determine  
193 whether larvae mutant for each individual *Pvf* exhibit defects in macrophage number. For  
194 *Pvf1*, a validated null allele (*Pvf1*<sup>1624</sup>) was available (27), however this was not the case for  
195 *Pvf2* or *Pvf3*. We therefore generated null mutants for each of these genes by making use of  
196 available lines carrying MiMIC transposons inserted within their introns (Figure 1A). The  
197 MiMIC transposon arrests transcription when inserted in the correct orientation (41) and can  
198 be replaced with a variety of available cassettes by recombinase-mediated cassette exchange  
199 (RMCE) (32). For *Pvf2* the insertion (*Pvf2*<sup>Mi00770</sup>) was incorrectly orientated, so we replaced  
200 the MiMIC transposon with a T2A-GAL4 cassette, which is intended to halt *Pvf2*  
201 transcription and instead produce GAL4 (*Pvf2*<sup>T2A-GAL4</sup>). The transposon located in *Pvf3*  
202 (*Pvf3*<sup>Mi04168</sup>, called *Pvf3*<sup>MiMIC</sup> here) was in the correct orientation and therefore expected to  
203 disrupt the gene. However, for the added utility of having a GAL4 reporter, we also replaced  
204 this with the T2A-GAL4 cassette (*Pvf3*<sup>T2A-GAL4</sup>). These insertions (MiMIC and T2A-GAL4)  
205 affect all known isoforms of *Pvf2* and *Pvf3* and likely truncate residual gene products to short  
206 fragments lacking their predicted receptor-binding PDGF domains (Figure 1A). Quantitative  
207 RT-PCR for the presence of exons downstream of the insertion sites in mutant larvae  
208 carrying the *Pvf2*<sup>T2A-GAL4</sup> and *Pvf3*<sup>MiMIC</sup> alleles confirmed that full-length transcripts are not  
209 detectable in the mutant lines (Figure 1B, C), indicating that these are likely null alleles.

210           Since macrophages represent >90% of the total population of blood cells, we next  
211           quantified total blood cells (circulating and tissue-resident) as a read out of macrophage  
212           number in *Pvf1-3* mutant larvae. As *Pvf1* is on the X chromosome we examined larvae  
213           hemizygous for the *Pvf1*<sup>1624</sup> allele and found no defects in larval blood cell number  
214           (*hmlΔdsRed*; Figure 1D;  $p>0.999$ ). In contrast, homozygous *Pvf2*<sup>T2A-GAL4</sup> and  
215           transheterozygous *Pvf2*<sup>T2A-GAL4</sup>/*df*<sup>BSC291</sup> larvae (where *df*<sup>BSC291</sup> is a deficiency allele that  
216           deletes a number of genes including *Pvf2* and *Pvf3*, used to eliminate genetic background  
217           effects) both had less than one third the number of blood cells of the heterozygote controls  
218           (*hmlΔdsRed*; Figure 1E, F; for *Pvf2*<sup>T2A-GAL4</sup>,  $p<0.001$  compared to *Pvf2*<sup>T2A-GAL4</sup>/+; for *Pvf2*<sup>T2A-</sup>  
219           *GAL4*/*df*<sup>BSC291</sup>,  $p<0.001$  compared to both *Pvf2*<sup>T2A-GAL4</sup>/+ and *df*<sup>BSC291</sup>/+). Similarly,  
220           homozygous *Pvf3*<sup>MiMIC</sup> (*hmlΔ-GAL4,UAS-GFP*), transheterozygous *Pvf3*<sup>MiMIC</sup>/*df*<sup>BSC291</sup> (*hmlΔ-*  
221           *GAL4,UAS-GFP*), and transheterozygous *Pvf3*<sup>MiMIC</sup>/*Pvf3*<sup>T2A-GAL4</sup> (*hmlΔdsRed*) larvae all  
222           exhibited large reductions in blood cell number compared to their respective heterozygous  
223           controls (Figure 1G-I, S1; for *Pvf3*<sup>MiMIC</sup>,  $p<0.001$  compared to *Pvf3*<sup>MiMIC</sup>/+; for  
224           *Pvf3*<sup>MiMIC</sup>/*df*<sup>BSC291</sup>,  $p<0.001$  compared to both *Pvf3*<sup>MiMIC</sup>/+ and *df*<sup>BSC291</sup>/+; for  
225           *Pvf3*<sup>MiMIC</sup>/*Pvf3*<sup>T2A-GAL4</sup>,  $p<0.001$  compared to *Pvf3*<sup>T2A-GAL4</sup>/+ and  $p=0.013$  compared to  
226           *Pvf3*<sup>MiMIC</sup>/*Pvf3*<sup>T2A-GAL4</sup>). Together, these data indicate that *Pvf2* and *Pvf3*, but not *Pvf1*,  
227           influence larval blood cell number in a non-redundant manner. Given the magnitude of these  
228           reductions in blood cell number, it is likely that they predominantly reflect reductions to  
229           numbers of macrophages.

230           While quantifying *Pvf3*<sup>MiMIC</sup>/*df*<sup>BSC291</sup> larvae, we noticed that *df*<sup>BSC291</sup>/+ control larvae  
231           had significantly fewer blood cells compared to *Pvf3*<sup>MiMIC</sup>/+ controls (Figure 1I,  $p=0.019$ )  
232           and wondered whether this was because of haploinsufficiency for *Pvf2*. In support of this  
233           idea, we found that *Pvf2*<sup>T2A-GAL4</sup>/+ individuals, which have ~50% reduction in *Pvf2* transcript  
234           (Figure 1B), also have significantly reduced blood cell numbers compared to the wildtype

235 control (Figure 1J,  $p=0.013$ ). Unlike  $Pvf2^{T2A-GAL4}$  heterozygotes,  $Pvf3^{MiMIC}/+$  larvae had a  
236 similar number of blood cells compared to wildtype controls (Figure 1H,  $p=0.336$ ), despite  
237 similarly having a reduction in  $Pvf3$  transcript levels compared to wildtype animals (Figure  
238 1C). This indicates that larval macrophage numbers may be more sensitive to dosage of  $Pvf2$   
239 than  $Pvf3$ .

240 We also surveyed the crystal cell population to see if it was affected. We found  
241 crystal cell numbers to be strongly reduced in  $Pvf2^{T2A-GAL4}$  and  $Pvf3^{MiMIC}$  homozygotes, as  
242 well as in transheterozygotes of these alleles with the  $df^{BSC291}$  allele (Figure S2A-E). These  
243 data strongly implicate  $Pvf2$  and  $Pvf3$  in the control of crystal cell numbers. Since crystal  
244 cells transdifferentiate directly from macrophages during the larval stage (23), this is the  
245 likely the result of a compromised macrophage population in  $Pvf2$  and  $Pvf3$  mutants, rather  
246 than a separate role in crystal cells.

247

#### 248 $Pvf2$ is required for larval macrophage self-renewal

249  $Pvr$  is required for the survival of embryonic blood cells and has been proposed to be  
250 activated by all Pvfs in this role (28, 42, 43), however their relative contributions have not  
251 been resolved. The decreased number of macrophages in  $Pvf2$  and  $Pvf3$  mutant larvae could  
252 therefore be due to defects in the hematopoiesis that occurs in the embryo to establish the  
253 initial macrophage population in early larvae. Alternatively, the reduction could be due to  
254 defects in the self-renewal that occurs later in larval macrophages, or to reductions in both.

255 To determine which of these possibilities is occurring we therefore assessed blood  
256 cell numbers in first instar larvae ( $hml\Delta dsRed$ ), prior to the major macrophage self-renewal  
257 period and thus where blood cell numbers are determined by embryonic hematopoiesis.  
258  $Pvf2^{T2A-GAL4}/Pvf2^{T2A-GAL4}$  larvae exhibited no defects in blood cell number at this stage (Figure  
259 2A,  $p=0.328$ ). In contrast,  $Pvf3^{MiMIC}/Pvf3^{T2A-GAL4}$  larvae had approximately half the number of

260 blood cells compared to their heterozygous controls (Figure 2B, compared to  $Pvf3^{MiMIC}/+$ :  
261  $p < 0.001$ ; to  $Pvf3^{T2A-GAL4}/+$ :  $p = 0.005$ ). When we estimated blood cell expansion rates using  
262 these data together with data from late stage larvae, we found no difference between  
263  $Pvf3^{MiMIC}/Pvf3^{T2A-GAL4}$  larvae and heterozygous controls (Figure S3A; Table S1), indicating  
264 that the phenotype observed in  $Pvf3$  mutants is solely due to an earlier role. Together, these  
265 data strongly suggest that Pvr signalling via Pvf2 but not Pvf3 mediates macrophage  
266 population expansion during the larval period.

267         Due to our interest in macrophage self-renewal, we focussed our attention on  
268 investigating how  $Pvf2$  controls the larval macrophage population. We reasoned that  $Pvf2$   
269 may achieve this by promoting macrophage survival and/or self-renewal. To assess survival,  
270 we measured apoptosis in  $Pvf2$  mutants early during the third instar stage when cell numbers  
271 are rapidly increasing. While the overall occurrence of blood cell death was very low at this  
272 stage in both  $Pvf2^{T2A-GAL4}$  homozygotes and heterozygous controls (0-1.2%), the effect was  
273 significantly greater upon loss of  $Pvf2$  (Figure 2C;  $p = 0.045$ ). However, such low levels of  
274 cell death were unlikely to explain the severe reduction in macrophages that we observed in  
275  $Pvf2$  mutants, so we suspected that there was a self-renewal deficit. We therefore assessed the  
276 rate of cell cycle progression by determining the rate at which blood cells incorporate the  
277 thymidine analogue EdU. Blood cells in  $Pvf2^{T2A-GAL4}$  homozygotes exhibited a marked and  
278 significant reduction in self-renewal rates (37%; Figure 2D;  $p = 0.029$ ). This aligns closely  
279 with the reduced blood cell expansion rate calculated by combining data from early and late  
280 stage larvae (35%, Figure S3B). We therefore conclude that  $Pvf2$  predominantly drives the  
281 expansion of the larval macrophage population by promoting their self-renewal.

282         Macrophage population expansion can be affected by both the accumulation of blood  
283 cells in hematopoietic pockets and by overall organismal growth (13, 38, 44). We therefore  
284 tested if the reduction in macrophage number in  $Pvf2$  mutants could be due to defects in one

285 of these processes. Defects in blood cell accumulation alter the relative proportion of blood  
286 cells in circulation (25), so we assessed this proportion in  $Pvf2^{T2A-GAL4}/df^{BSC291}$   
287 transheterozygotes. We found that the relative proportions of tissue-resident to circulating  
288 blood cells did not differ from heterozygous controls (Figure S4A). In addition,  $Pvf2$  mutant  
289 animals were not growth-impaired (Figure S4B) and their ability to coordinate blood cell  
290 numbers with body size was also not affected (Figure S4C; Table S2). These data suggest  
291 that  $Pvf2$  may regulate the self-renewal process via a novel mechanism.

292

### 293 A subpopulation of blood cells express $Pvf2$ for macrophage self-renewal

294 To better understand how  $Pvf2$  influences macrophage self-renewal, we next  
295 investigated the tissue/ cellular origin(s) of  $Pvf2$  for this role. For this we used the  $Pvf2^{T2A-}$   
296  $GAL4$  allele to drive expression of a *YFP* reporter and explored whether  $Pvf2$  is expressed in  
297 blood cells. We first validated that the  $Pvf2^{T2A-GAL4}$  reporter faithfully reproduced the reported  
298 expression patterns of  $Pvf2$  (Figure S5A, B). We then tested for expression in larval blood  
299 cell populations by determining whether YFP ( $Pvf2^{T2A-GAL4}/+>UAS-YFP$ ) colocalises with  
300 dsRed (*hmlΔdsRed*) in larvae. This revealed a YFP signal that was significantly above  
301 background levels in a small number of both tissue-resident and circulating blood cells from  
302  $Pvf2^{T2A-GAL4}/+>UAS-YFP$  larvae (~1%, Figure 3A; for tissue-resident, p=0.001 compared to  
303 both  $Pvf2^{T2A-GAL4}/+$  and *UAS-YFP*; for circulating, p=0.019 compared to  $Pvf2^{T2A-GAL4}/+$  and  
304 p=0.010 compared to *UAS-YFP*). This was further confirmed by live-imaging, which showed  
305 that these cells, like other blood cells, are dispersed throughout the larva (Figure 3B, Movie  
306 1). Thus, the  $Pvf2$  required for larval macrophage self-renewal may be produced by the blood  
307 cells themselves.

308 Notably, we did not detect  $Pvf2$  expression in blood cells within the lymph gland  
309 (Figure S5C), suggesting that  $Pvf2$  expression may be restricted to blood cells of embryonic

310 origin. In agreement with this, when we looked at late-stage  $Pvf2^{T2A-GAL4/+>UAS-YFP}$   
311 embryos co-expressing an embryonic blood cell marker (*SrpHemo-H2A-mCherry*) (45), we  
312 consistently found several YFP-positive blood cells (~1-5 per embryo; Figure 3C, Movie 2).  
313 This indicates that these cells are present throughout the larval stage. Consistent with *Pvf3*  
314 not playing a role in self-renewal, we did not detect *Pvf3* expression in larval blood cells  
315 (Figure S6A-C).

316 To determine if blood cell-produced *Pvf2* is required for macrophage expansion, we  
317 knocked-down *Pvf2* expression specifically in larval blood cells via RNAi driven by *hml-*  
318 *GAL4*. This resulted in a significant reduction in larval blood cell number compared to the  
319 controls carrying *hml-GAL4* alone ( $p=0.001$ ; Figure 3D, S7). These data suggest that *Pvf2*  
320 expression in blood cells is important for macrophage self-renewal. Moreover, because  
321 ectopic *Pvf2* expression in all larval blood cells results in a striking overexpansion phenotype  
322 (Figure 3E,  $p<0.001$ ) (44), rates of macrophage self-renewal may be the product of not only  
323 *Pvf2* expression levels within blood cells, but also the number of blood cells that express  
324 *Pvf2*.

325

### 326 Blood cell *Pvf2* expression is transient

327 We were next interested to understand whether the observed *Pvf2* expression defines  
328 a novel lineage of *Drosophila* blood cells or instead represents a transient state. To address  
329 this, we performed a lineage tracing experiment where we used  $Pvf2^{T2A-GAL4}$  to drive  
330 expression of a photoconvertible green fluorescent protein (*UAS-EOS-GFP*) that is cleaved  
331 upon UV irradiation, causing it to emit light in the red spectrum (EOS-GFP<sup>RED</sup>; Figure 4A)  
332 (46).  $Pvf2^{T2A-GAL4/+>UAS-EOS-GFP}$  larvae were irradiated such that *Pvf2*-expressing  
333 macrophages and all their descendants are marked by EOS-GFP<sup>RED</sup>. Conversely, any cells  
334 that later switch on expression of *Pvf2* are marked by EOS-GFP alone (green). Live-imaging

335 24 hours after photoconversion revealed most *Pvf2*-expressing blood cells, but not other  
336 *Pvf2*-positive tissues (e.g. trachea), to express EOS-GFP alone (Figure 4B). These data  
337 suggest that blood cells can switch on *Pvf2* expression throughout the larval stage.

338 As an alternative means of testing whether *Pvf2* expression is transient, we performed  
339 a different lineage tracing experiment using the G-TRACE system (comprising *UAS-RFP*,  
340 *UAS-FLP* and *Ubi<sup>trp63</sup>-FRT-STOP-FRT-GFP* transgenes) (47) driven by *Pvf2<sup>T2A-GAL4</sup>*.  
341 Expression of FLP recombinase in *Pvf2*-expressing cells (marked by RFP) causes permanent  
342 expression of GFP in these cells and their descendants. Thus, here GFP is an indicator of  
343 previous expression and RFP an indicator of current or recent expression (Figure 4C).  
344 Extraction of the tissue-resident blood cells from *Pvf2<sup>T2A-GAL4/+>G-TRACE</sup>* larvae revealed  
345 the presence all combinations of RFP- and GFP-positive cells above background levels  
346 (Figure 4D, S8A, B). In particular, the presence of GFP-positive and RFP-negative blood  
347 cells in *Pvf2<sup>T2A-GAL4/+>G-TRACE</sup>* larvae strongly suggests that, during the larval stage, these  
348 cells cease expressing *Pvf2* ( $p=0.004$  compared to larvae carrying *G-TRACE* only and  
349  $p<0.001$  compared to *Pvf2<sup>T2A-GAL4/+>RFP</sup>*). These data thus support the idea that *Pvf2*-  
350 expression in blood cells is a transient event.

351

## 352 Discussion

353 Here we define a novel mechanism for the control of macrophage self-renewal in  
354 *Drosophila*, at the centre of which is the VEGF- and PDGF-related receptor (Pvr) signalling  
355 pathway. Pvr has been previously implicated in the control of blood cell number, however its  
356 contribution to their expansion in larvae and the nature of this have remained unknown (28,  
357 30, 31). We found that Pvr is controlled by one of the three known Pvr ligands in this role,  
358 Pvf2. Specifically, we show that *Pvf2* expression levels in circulating and tissue-resident  
359 larval blood cells controls the rate of macrophage self-renewal and, to a lesser extent, blood

360 cell survival. Our study however, does not rule out sources of *Pvf2* in tissues other than the  
361 blood cells. Indeed, we noted its expression in various tissues that may supply *Pvf2* to the  
362 lymph (e.g. trachea). However, we reason that the observed sensitivity of blood cells to more  
363 or less *Pvf2* argues strongly that the blood cells act as significant contributors to the pool of  
364 *Pvf2* required for macrophage self-renewal.

365 Most notably our data suggests that, while only a small percentage of blood cells  
366 express *Pvf2*, these cells do not represent a novel blood cell lineage. Instead, this expression  
367 pattern is maintained via the transient expression of *Pvf2* in blood cells. Consistent with our  
368 findings, single cell RNA-sequencing of larval blood cells has shown that only a small  
369 proportion of blood cells express *Pvf2* (~4%) and these cells do not cluster with any of the 16  
370 identified blood cell lineages (Figure S9) (48). Currently, it remains unknown what signal(s)  
371 controls *Pvf2* expression in blood cells. However, since *Pvf2* expression is observed in blood  
372 cells from late embryogenesis and throughout the larval stage, the signal(s) that activates  
373 *Pvf2* expression is likely present during all of these stages. Whether this signal can influence  
374 *Pvf2*-expression in response to environmental stresses (e.g. infection, wounding) to modulate  
375 macrophage number is yet to be determined.

376 We have also shown that *Pvf3* determines the final macrophage population size.  
377 However, our data suggests that, unlike *Pvf2*, *Pvf3* is required prior to the onset of the larval  
378 stage and does not control larval macrophage self-renewal. In the embryo, *Pvr* influences  
379 blood cell numbers by promoting their survival, with genetic removal of *Pvr* resulting in up  
380 to 70% fewer blood cells (28). Although several studies have proposed that all *Pvr* ligands  
381 are required for the survival of embryonic blood cells, this has not been confirmed via the use  
382 of single *Pvf1-3* mutants (28, 42, 43). Our assessment of single mutants for *Pvf2* and *Pvf3*  
383 early during the larval stage revealed that *Pvf3* mutants exhibit a similar reduction in blood  
384 cell number to *Pvr* mutants (~50%). In addition, the data reported here and the single cell



385 RNA-sequencing conducted by Tattikotta et al. revealed that negligible numbers of larval  
386 blood cells express *Pvf3* (Figure S9) (48). Instead, *Pvf3* is more highly expressed in  
387 embryonic blood cells than larval blood cells (49). Together, these data suggest that *Pvf3*  
388 alone is likely responsible for Pvr-mediated blood cell survival in embryos.

389 Our data further suggests that the transition from embryonic to larval hematopoiesis  
390 involves a switch in Pvr function from supporting macrophage survival to promoting their  
391 self-renewal. Interestingly, this switch coincides with a change in the ligand that activates  
392 Pvr. What purpose the shifting of ligands serves to this and whether the promotion of larval  
393 macrophage survival has been relegated to another pathway (such as the Toll pathway) (50)  
394 remain interesting questions.

395 The data presented here describes and underscores the importance of the Pvr  
396 signalling pathway as a central regulator of *Drosophila* hematopoiesis. Importantly, our data  
397 reveal a new mechanism for how macrophage self-renewal can be regulated involving  
398 PDGF/VEGF receptor signalling. Members of these signalling pathways including the  
399 PDGFR-like colony stimulating factor receptor 1, and more recently VEGF-C, have been  
400 implicated in macrophage self-renewal in vertebrates (4, 51, 52). The strong similarities  
401 between *Drosophila* and vertebrates in this regard suggest that these cell signalling pathways  
402 likely have ancient evolutionary origins in the control of macrophage self-renewal. Indeed it  
403 will be interesting to learn the extent to which this is true and the degree to which regulatory  
404 mechanisms are conserved across distant animal species.

405

406

#### 407 **Acknowledgments**

408 We thank the Australian *Drosophila* Biomedical Research Facility (OzDros) and Monash  
409 Micro Imaging for technical support. In addition, we thank the Bloomington *Drosophila*

410 Stock Centre, Kyoto Stock Centre, and Katja Brückner for fly stocks, Linda Parsons, Tim  
411 Connallon, Christen Mirth and Grace Jefferies for advice and critical reading of the  
412 manuscript. J.C.W. is an Australian Research Council Laureate Fellow. This work was  
413 further supported by the Monash University Science-Medicine, Nursing, and Health Science  
414 Faculties Interdisciplinary Research Scheme.

415 **Figure and movie legends**

416 **Figure 1. *Pvf2* and *Pvf3*, but not *Pvf1* influence larval blood cell number.**

417 (A) *Pvf2-3* genomic region and transcripts. Transcriptional start sites are indicated by arrows,  
418 boxes denote exons (coding sequence is filled with blue denoting PDGF domain sequences),  
419 and the positions of two relevant MiMIC transposons are shown. Relative transcript levels of  
420 *Pvf2* (B) and *Pvf3* (C) in larvae of the genotypes indicated shows that *Pvf2*<sup>T2A-GAL4</sup> the  
421 *Pvf3*<sup>MiMIC</sup> alleles fail to produce detectable transcript levels of *Pvf2* and *Pvf3*, respectively.  
422 (D) *Pvf1*<sup>1624/Y</sup> larvae exhibited no significant difference in their total blood cell number  
423 compared to wild-type controls ( $p > 0.999$ , *hmlΔdsRed*,  $n \geq 4$ ). (E) *Pvf2*<sup>T2A-GAL4</sup>/*Pvf2*<sup>T2A-GAL4</sup>  
424 larvae appear to have fewer blood cells (*hmlΔdsRed*) than *Pvf2*<sup>T2A-GAL4/+</sup> controls. (F) Blood  
425 cells numbers in homozygous *Pvf2*<sup>T2A-GAL4</sup> and *Pvf2*<sup>T2A-GAL4/df<sup>BSC291</sup></sup> larvae are strongly  
426 reduced compared to heterozygous controls (*hmlΔdsRed*,  $n = 8$ ). (G) *Pvf3*<sup>MiMIC</sup>/*Pvf3*<sup>MiMIC</sup>  
427 larvae appear to have fewer blood cells (*hmlΔ-GAL4 > UAS-GFP*) than *Pvf3*<sup>MiMIC/+</sup> controls.  
428 This was confirmed by blood cell quantification of *Pvf3*<sup>MiMIC</sup>/*Pvf3*<sup>MiMIC</sup> (H) and  
429 *Pvf3*<sup>MiMIC/df<sup>BSC291</sup></sup> (I) larvae compared to heterozygous controls (*hmlΔ-GAL4 > UAS-GFP*,  
430  $n \geq 7$ ). (J) *Pvf2*<sup>T2A-GAL4/+</sup> heterozygotes have fewer blood cells than wildtype larvae  
431 (*hmlΔdsRed*,  $n = 8$ ). ns: not significant, lowercase letters indicate genotypes that differ  
432 significantly by an unpaired t-test with Welch's correction (B-C) or a Mann-Whitney test (D-  
433 J). Data points are individual larvae with means plotted  $\pm 1$  standard error. Scale bars are  
434 1mm.

435

436 **Figure 2. *Pvf2* mediates larval macrophage self-renewal**

437 Total blood cell numbers in *Pvf2*<sup>T2A-GAL4</sup>/*Pvf2*<sup>T2A-GAL4</sup> (A) and *Pvf3*<sup>MiMIC</sup>/*Pvf3*<sup>T2A-GAL4</sup> (B)  
438 larvae at the first instar stage. While *Pvf2*<sup>T2A-GAL4</sup>/*Pvf2*<sup>T2A-GAL4</sup> larvae were not different from  
439 the heterozygous controls ( $n = 8$ ), *Pvf3*<sup>MiMIC</sup>/*Pvf3*<sup>T2A-GAL4</sup> larvae had markedly fewer blood

440 cells (*hmlΔdsRed*,  $n \geq 5$ ). (C) The percentage of TUNEL-positive blood cells is higher in  
441 *Pvf2<sup>T2A-GAL4</sup>/Pvf2<sup>T2A-GAL4</sup>* larvae compared to heterozygous controls ( $n \geq 8$ ). (D) Rates of blood  
442 cell DNA replication (EdU incorporation) are strongly reduced in *Pvf2<sup>T2A-GAL4</sup>/Pvf2<sup>T2A-GAL4</sup>*  
443 larvae compared to heterozygous controls ( $n \geq 9$ ). ns: not significant, lowercase letters indicate  
444 genotypes that differ significantly by a Mann-Whitney test. Data points are individual larvae  
445 with means plotted  $\pm 1$  standard error.

446

447 **Figure 3. *Pvf2* expression in a blood cell subpopulation drives self-renewal.**

448 (A) Less than 1% of circulating and tissue-resident blood cells from *Pvf2<sup>T2A-GAL4</sup>/+>UAS-*  
449 *YFP* larvae express YFP above background levels (*Pvf2<sup>T2A-GAL4</sup>/+* and *UAS-YFP* alone,  $n \geq 5$ ).  
450 (B) Representative still image of the posterior-dorsal side of a live third instar *Pvf2<sup>T2A-</sup>*  
451 *GAL4/+>UAS-YFP* larva showing blood cells (*hmlΔdsRed*) including several that express YFP  
452 (arrowed). (C) Late-stage *Pvf2<sup>T2A-GAL4</sup>/+>UAS-YFP* embryo (anti-GFP to visualise YFP)  
453 showing a small number of blood cells (*SrpHemo-H2A-mCherry*, nuclear) that colocalise  
454 with the YFP signal. Magnifications of three YFP-positive blood cells are shown below (C'-  
455 C'''). (D) Larvae expressing *Pvf2 RNAi* in all larval blood cells (*hml-GAL4>UAS-GFP*)  
456 exhibit a reduction in blood cell number ( $n \geq 15$ ). (E) Overexpression of *Pvf2* in all larval  
457 blood cells (*hml-GAL4>UAS-GFP*) strikingly increases in circulating blood cell number  
458 ( $n = 8$ ). Lowercase letters indicate genotypes that differ significantly by a Mann-Whitney test.  
459 Data points are individual larvae with means plotted  $\pm 1$  standard error. Scale bars are 50  $\mu\text{m}$ .

460

461 **Figure 4. *Pvf2* expression in larval blood cells is a transient event.**

462 (A) Schematic of the EOS-GFP experiment. EOS-GFP (B, green channel) and UV-converted  
463 EOS-GFP (B', EOS-GFP<sup>RED</sup>, red channel, overexposed) on the posterior-dorsal side of a live  
464 *Pvf2<sup>T2A-GAL4</sup>/+>UAS-EOS-GFP* larva 24 hours post-UV irradiation. Note that the blood cells

465 contain EOS-GFP only, whereas the trachea (arrowed) also has EOS-GFP<sup>RED</sup>. (C) Schematic  
466 for the G-TRACE experiment. (D) Quantification of tissue-resident blood cells from *Pvf2*<sup>T2A-</sup>  
467 <sup>GAL4</sup> /+, *Pvf2*<sup>T2A-GAL4</sup> /+>*RFP* and *Pvf2*<sup>T2A-GAL4</sup> /+>*G-TRACE* larvae. Larvae carrying both  
468 *Pvf2*<sup>T2A-GAL4</sup> /+ and *G-TRACE* have RFP- and/ or GFP-positive blood cells that are above  
469 background levels (defined using controls not expressing the relevant fluorescent proteins;  
470 for RFP<sup>+</sup>GFP<sup>-</sup>, p=0.004 compared to larvae carrying *G-TRACE* alone; for RFP<sup>-</sup>GFP<sup>+</sup>,  
471 p=0.004 compared to larvae carrying *G-TRACE* alone and p<0.001 compared to *Pvf2*<sup>T2A-</sup>  
472 <sup>GAL4</sup> /+>*RFP* larvae; for RFP<sup>+</sup>GFP<sup>+</sup>, p=0.004 compared to larvae carrying *G-TRACE* alone  
473 and p=0.003 compared to *Pvf2*<sup>T2A-GAL4</sup> /+>*RFP* larvae). The presence of GFP<sup>-</sup>RFP<sup>+</sup> and  
474 GFP<sup>+</sup>RFP<sup>-</sup> blood cells from *Pvf2*<sup>T2A-GAL4</sup> /+>*G-TRACE* larvae indicates that the cells either  
475 currently express *Pvf2*, or previously expressed *Pvf2* and since have ceased, respectively.  
476 Lowercase letters indicate genotypes that differ significantly by a Mann-Whitney test for a  
477 given colour combination. Data points are individual larvae with means plotted ±1 standard  
478 error. Scale bars are 50µm.

479

#### 480 **Movie 1.**

481 A third instar *Pvf2*<sup>T2A-GAL4</sup> >*UAS-YFP* larva with blood cells marked by *hmlΔdsRed*. Several  
482 YFP-expressing blood cells (yellow) are visible. Frames were captured at 30 second intervals  
483 for 58 minutes.

484

#### 485 **Movie 2.**

486 A late-stage *Pvf2*<sup>T2A-GAL4</sup> >*UAS-YFP* embryo with blood cells marked by *SrpHemo-H2A-*  
487 *mCherry*. Note the YFP-positive blood cell indicated by an asterisk. Frames were captured at  
488 2-minute intervals for one hour.

489 **References**

- 490 1. L. C. Davies, S. J. Jenkins, J. E. Allen, P. R. Taylor, Tissue-resident macrophages.  
491 *Nature Immunology* **14**, 986-995 (2013).
- 492 2. T. A. Wynn, A. Chawla, J. W. Pollard, Macrophage biology in development,  
493 homeostasis and disease. *Nature* **496**, 445-455 (2013).
- 494 3. U. Banerjee, J. G. Girard, L. M. Goins, C. M. Spratford, *Drosophila* as a Genetics  
495 Model for Hematopoiesis. *Genetics* **211**, 367-417 (2019).
- 496 4. C. V. Jones, S. D. Ricardo, Macrophages and CSF-1: Implications for development  
497 and beyond. *Organogenesis* **9**, 249-260 (2013).
- 498 5. I. Anderl *et al.*, Transdifferentiation and Proliferation in Two Distinct Hemocyte  
499 Lineages in *Drosophila melanogaster* Larvae after Wasp Infection. *PLoS Pathogens*  
500 **12**, (2016).
- 501 6. R. Lanot, D. Zachary, F. Holder, M. Meister, Postembryonic hematopoiesis in  
502 *Drosophila*. *Developmental Biology* **230**, 243-257 (2001).
- 503 7. M. H. Sieweke, J. E. Allen, Beyond stem cells: Self-renewal of differentiated  
504 macrophages. *Science* **342**, (2013).
- 505 8. W. T'Jonck, M. Guilliams, J. Bonnardel, Niche signals and transcription factors  
506 involved in tissue-resident macrophage development. *Cellular Immunology* **330**, 43-  
507 53 (2018).
- 508 9. T. Röszer, Understanding the Biology of Self-Renewing Macrophages. *Cells* **7**, 103  
509 (2018).
- 510 10. S. Epelman, K. J. Lavine, G. J. Randolph, Origin and Functions of Tissue  
511 Macrophages. *Immunity* **41**, 21-35 (2014).
- 512 11. K. S. Gold, K. Bruckner, *Drosophila* as a model for the two myeloid blood cell  
513 systems in vertebrates. *Experimental Hematology* **42**, 717-727 (2014).

- 514 12. U. Tepass, L. I. Fessler, A. Aziz, V. Hartenstein, Embryonic origin of hemocytes and  
515 their relationship to cell-death in *Drosophila*. *Development* **120**, 1829-1837 (1994).
- 516 13. K. Makhijani, B. Alexander, T. Tanaka, E. Rulifson, K. Brückner, The peripheral  
517 nervous system supports blood cell homing and survival in the *Drosophila* larva.  
518 *Development* **138**, 5379-5391 (2011).
- 519 14. S. H. Jung, C. J. Evans, C. Uemura, U. Banerjee, The *Drosophila* lymph gland as a  
520 developmental model of hematopoiesis. *Development* **132**, 2521-2533 (2005).
- 521 15. T. M. Rizki, R. M. Rizki, Lamellocyte differentiation in *Drosophila* larvae parasitized  
522 by *Leptopilina*. *Developmental and Comparative Immunology* **16**, 103-110 (1992).
- 523 16. Y. Carton, M. Bouletreau, J. J. M. van Alphen, J. C. van Lenteren, “The *Drosophila*  
524 parasitic wasps” in *The genetics and biology of Drosophila* **3e**, (1986), pp. 347-394.
- 525 17. C. J. Evans, V. Hartenstein, U. Banerjee, Thicker than blood: Conserved mechanisms  
526 in *Drosophila* and vertebrate hematopoiesis. *Developmental Cell* **5**, 673-690 (2003).
- 527 18. P. Sanchez Bosch *et al.*, Adult *Drosophila* Lack Hematopoiesis but Rely on a Blood  
528 Cell Reservoir at the Respiratory Epithelia to Relay Infection Signals to Surrounding  
529 Tissues. *Developmental Cell* **51**, 787-803.e785 (2019).
- 530 19. A. Holz, B. Bossinger, T. Strasser, W. Janning, R. Klapper, The two origins of  
531 hemocytes in *Drosophila*. *Development* **130**, 4955-4962 (2003).
- 532 20. T. Lebestky, T. Chang, V. Hartenstein, U. Banerjee, Specification of *Drosophila*  
533 hematopoietic lineage by conserved transcription factors. *Science* **288**, 146-149  
534 (2000).
- 535 21. V. Honti *et al.*, Cell lineage tracing reveals the plasticity of the hemocyte lineages and  
536 of the hematopoietic compartments in *Drosophila melanogaster*. *Molecular*  
537 *Immunology* **47**, 1997-2004 (2010).

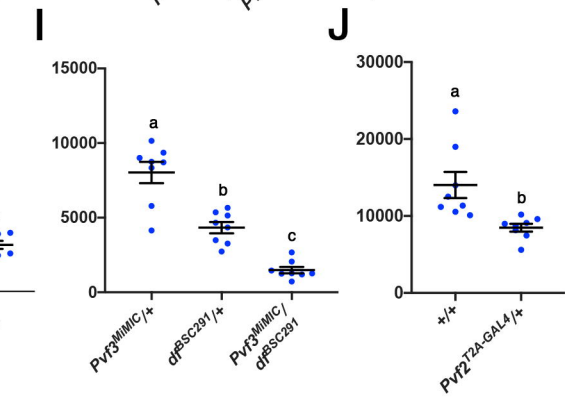
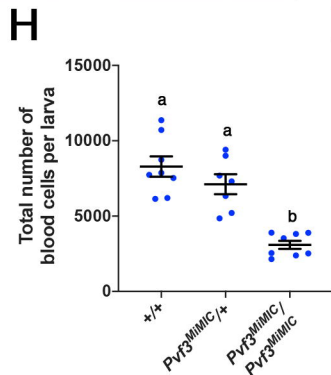
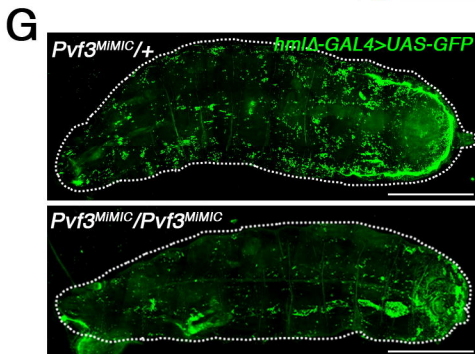
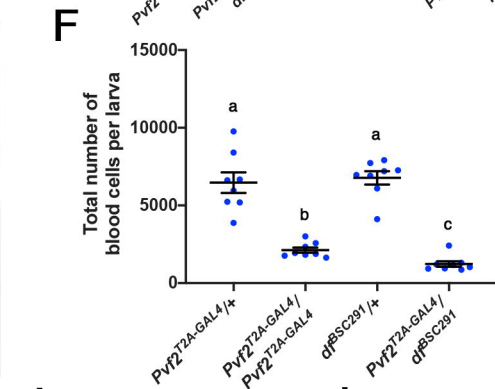
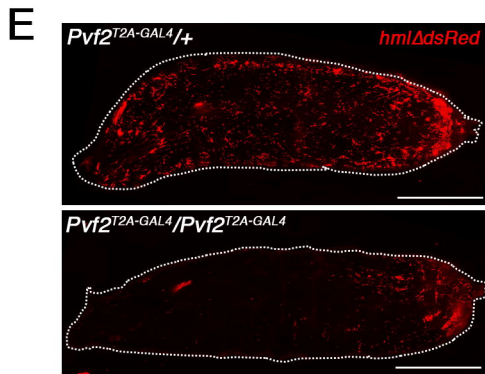
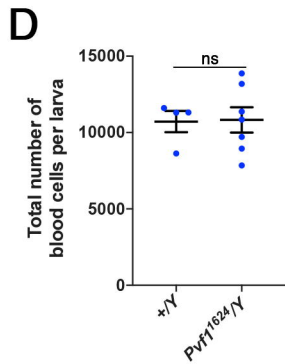
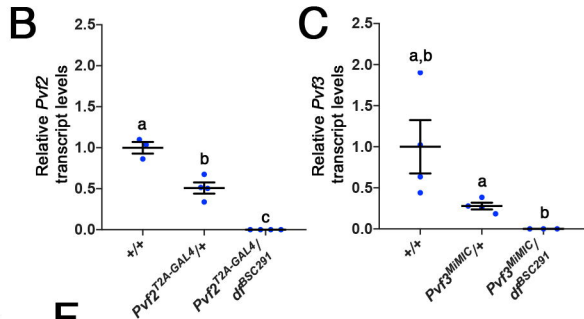
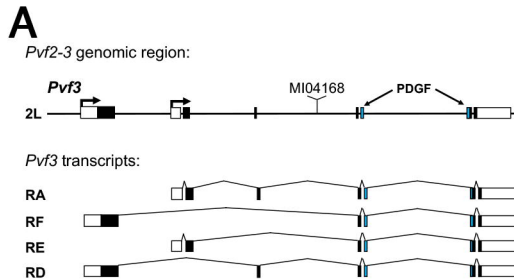
- 538 22. S. Petraki, B. Alexander, K. Brückner, Assaying Blood Cell Populations of the  
539 *Drosophila melanogaster* Larva. *Jove-Journal of Visualized Experiments*, 11 (2015).
- 540 23. A. B. Leitao, E. Sucena, *Drosophila* sessile hemocyte clusters are true hematopoietic  
541 tissues that regulate larval blood cell differentiation. *Elife* **4**, e06166 (2015).
- 542 24. M. Grigorian, L. Mandal, V. Hartenstein, Hematopoiesis at the onset of  
543 metamorphosis: terminal differentiation and dissociation of the *Drosophila* lymph  
544 gland. *Development Genes and Evolution* **221**, 121-131 (2011).
- 545 25. K. Makhijani *et al.*, Regulation of *Drosophila* hematopoietic sites by Activin- $\beta$  from  
546 active sensory neurons. *Nature Communications* **8**, 15990 (2017).
- 547 26. T. I. Heino *et al.*, The *Drosophila* VEGF receptor homolog is expressed in hemocytes.  
548 *Mechanisms of Development* **109**, 69-77 (2001).
- 549 27. P. Duchek, K. Somogyi, G. Jékely, S. Beccari, P. Rørth, Guidance of Cell Migration  
550 by the *Drosophila* PDGF/VEGF Receptor. *Cell* **107**, 17-26 (2001).
- 551 28. K. Brückner *et al.*, The PDGF/VEGF Receptor Controls Blood Cell Survival in  
552 *Drosophila*. *Developmental Cell* **7**, 73-84 (2004).
- 553 29. A. I. Munier *et al.*, PVF2, a PDGF/VEGF-like growth factor, induces hemocyte  
554 proliferation in *Drosophila* larvae. *Embo Reports* **3**, 1195-1200 (2002).
- 555 30. T. A. Tran *et al.*, Platelet-Derived Growth Factor/Vascular Endothelial Growth Factor  
556 Receptor Inactivation by Sunitinib Results in Tsc1/Tsc2-Dependent Inhibition of  
557 TORC1. *Molecular and Cellular Biology* **33**, 3762-3779 (2013).
- 558 31. C. J. Zettervall *et al.*, A directed screen for genes involved in *Drosophila* blood cell  
559 activation. *Proceedings of the National Academy of Sciences of the United States of*  
560 *America* **101**, 14192-14197 (2004).
- 561 32. F. Diao *et al.*, Plug-and-play genetic access to *drosophila* cell types using  
562 exchangeable exon cassettes. *Cell Reports* **10**, 1410-1421 (2015).

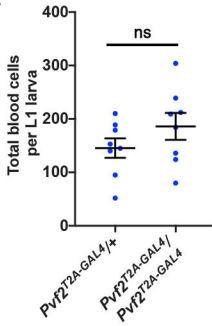
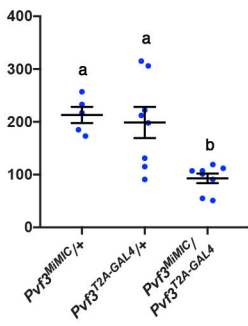
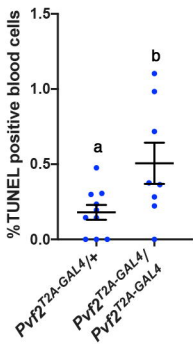


- 563 33. O. J. Marshall, PerlPrimer: Cross-platform, graphical primer design for standard,  
564 bisulphite and real-time PCR. *Bioinformatics* **20**, 2471-2472 (2004).
- 565 34. J. E. Collinge, A. R. Anderson, A. R. Weeks, T. K. Johnson, S. W. McKechnie,  
566 Latitudinal and cold-tolerance variation associate with DNA repeat-number variation  
567 in the hsr-omega RNA gene of *Drosophila melanogaster*. *Heredity* **101**, 260-270  
568 (2008).
- 569 35. A. Goto, T. Kadowaki, Y. Kitagawa, *Drosophila* hemolectin gene is expressed in  
570 embryonic and larval hemocytes and its knock down causes bleeding defects.  
571 *Developmental Biology* **264**, 582-591 (2003).
- 572 36. S. A. Sinenko, B. Mathey-Prevot, Increased expression of *Drosophila* tetraspanin,  
573 Tsp68C, suppresses the abnormal proliferation of ytr-deficient and Ras/Raf-activated  
574 hemocytes. *Oncogene* **23**, 9120-9128 (2004).
- 575 37. J. Schindelin *et al.*, Fiji: An open-source platform for biological-image analysis.  
576 *Nature Methods* **9**, 676-682 (2012).
- 577 38. D. Bakopoulos *et al.*, Insulin-Like Signalling Influences the Coordination of Larval  
578 Hemocyte Number with Body Size in *Drosophila melanogaster*. *G3: Genes,*  
579 *Genomes, Genetics* **10**, 2213-2220 (2020).
- 580 39. L. Forbes-Beadle *et al.*, Development of the cellular immune system of *Drosophila*  
581 requires the Membrane Attack Complex/Perforin-like protein Torso-like. *Genetics*  
582 **204**, 675-681 (2016).
- 583 40. A. L. Daul, H. Komori, C. Y. Lee, Edu (5-ethynyl-2'-deoxyuridine) labeling of  
584 *Drosophila* mitotic neuroblasts. *Cold Spring Harbor Protocols* **5**, (2010).
- 585 41. K. J. T. Venken *et al.*, MiMIC: A highly versatile transposon insertion resource for  
586 engineering *Drosophila melanogaster* genes. *Nature Methods* **8**, 737-747 (2011).

- 587 42. B. Parsons, E. Foley, The Drosophila Platelet-derived Growth Factor and Vascular  
588 Endothelial Growth Factor-Receptor Related (Pvr) Protein Ligands Pvf2 and Pvf3  
589 Control Hemocyte Viability and Invasive Migration. *Journal of Biological Chemistry*  
590 **288**, 20173-20183 (2013).
- 591 43. W. Wood, C. Faria, A. Jacinto, Distinct mechanisms regulate hemocyte chemotaxis  
592 during development and wound healing in *Drosophila melanogaster*. *Journal of Cell*  
593 *Biology* **173**, 405-416 (2006).
- 594 44. E. Ramond *et al.*, The adipokine NimrodB5 regulates peripheral hematopoiesis in  
595 *Drosophila*. *The FEBS Journal*, (2020).
- 596 45. A. Gyoergy *et al.*, Tools allowing independent visualization and genetic manipulation  
597 of *Drosophila melanogaster* macrophages and surrounding tissues. *G3: Genes,*  
598 *Genomes, Genetics* **8**, 845-857 (2018).
- 599 46. O. V. Stepanenko *et al.*, Modern fluorescent proteins: From chromophore formation  
600 to novel intracellular applications. *BioTechniques* **51**, 313-327 (2011).
- 601 47. C. J. Evans *et al.*, G-TRACE: Rapid Gal4-based cell lineage analysis in *Drosophila*.  
602 *Nature Methods* **6**, 603-605 (2009).
- 603 48. S. G. Tattikota *et al.*, A single-cell survey of drosophila blood. *eLife* **9**, 1-35 (2020).
- 604 49. P. B. Cattenoz *et al.*, Temporal specificity and heterogeneity of *Drosophila* immune  
605 cells. *EMBO Journal* **39**, (2020).
- 606 50. N. Matova, K. V. Anderson, Rel/NF- $\kappa$ B double mutants reveal that cellular immunity  
607 is central to *Drosophila* host defense. *Proceedings of the National Academy of*  
608 *Sciences of the United States of America* **103**, 16424-16429 (2006).
- 609 51. S. Fang *et al.*, Critical requirement of VEGF-C in transition to fetal erythropoiesis.  
610 *Blood* **128**, 710-720 (2016).

611 52. F. G. Brunet, J. N. Volf, M. Scharl, Whole genome duplications shaped the receptor  
612 tyrosine kinase repertoire of jawed vertebrates. *Genome Biology and Evolution* **8**,  
613 1600-1613 (2016).  
614  
615



**A****B****C****D**